Statistical characterization of images – Anisotropy

H.N. Teodorescu

Romanian Academy – Iasi Branch
Carol I nr. 8 Iasi
And Gheorghe Asachi Technical University of Iasi
Iasi, Romania

L. Dascalescu

Electrostatics of Dispersed Media Research Unit,
Electrohydrodynamics Group, P'Institute, UPR3346,
CNRS-University of Poitiers-ENSMA, IUT
d'Angoulême, 16021, Angoulême, France

*Abstract –*The purposes of the paper are to contribute to the understanding of the notion of anisotropy of images and to expose details on a method for deriving global and local statistical features on materials, based on anisotropy. We introduce a definition of anisotropy related to the edges and improve measures of anisotropy. The images dealt with correspond mainly to non-woven fabrics based on polymeric fibers. A discussion of the applicative potential is included.

Keywords- statistical properties; image processing; optical properties; non-woven fabrics; electrostatic filters

I. INTRODUCTION

To clarify the background of the problem, we start with the description of an application example. The interest in the global and local statistical properties of textiles relies in the potential improvement of the correlation between the optical and electrical charging properties, in view of founding an industrial, cheap, automated, indirect test method that would allow predicting the quality of the electrostatic dust filters based on non-woven materials. In contrast with the direct electrostatic measurements, the optical, indirect method is fast and suitable to deploy on the production line. The investigation in [1] primarily addressed the density of the polymeric material in the fabric. We hypothesize that the anisotropy of the fiber arrangement in the fabric may also play a role in the prediction of the electrostatic charging properties, hence the interest in statistically characterizing the anisotropy.

There are numerous approaches for defining image anisotropy. Many of these approaches derive directly from the classic paper by Kass and Witkin, [2]. Various methods for estimating anisotropy have been proposed. Brunet-Imbault et al. [3] use the FFT and then select manually the angular regions of integration of the bone (image) density, then compute the ratio of the result of the integration as an index. FFT-based methods are relatively intensive in respect to computation, but have the advantage of clearly indicating visually the preferred directions of the anisotropic structure, when the texture is highly anisotropic. A method for detecting anisotropy based on the comparison of small segments of the images was proposed by Keyhani et al. [4]. Nguyen et al. [5] have used the so called "conditional texture anisotropy" for finding the cracks in the pavement; their method jointly uses local brightness and connectivity, moreover transversal profile optical (brightness) measurements for assessing anisotropy in images – a method close to the one suggested in this paper. In another approach, Bierme and F. Richard [6] recall that orientation information can be determined based on line and projection processes of the image, then propose a model for the image consisting in the superposition of two stochastic processes, the extended fractional Brownian field and the Gaussian operator scaling field. Based on that model, they provide foundations for the anisotropy definition based on line and projection statistics. Their work is significant as a foundation for this study where projection statistics is used, as the current one. The same authors continue their previous work in [7] and [8]. Yet another approach is based on wavelets [9], while Gabarda and Cristóbal [10] propose the use of entropy for defining the anisotropy of images. In a paper performing an extensive comparison of various anisotropy calculations, Lehoucq et al. [11] use "the inertia tensor of the signal within a box", where a box can be of any predefined shape (circle, square); as the inertia tensor is asymmetric, it can be used to represent anisotropy.

The methods in this paper relate also to studies where derivative and directional filtering were used to define anisotropy, for example the early paper by van Vliet and Verbeek [12], where the gradient-square tensor is used to characterize the local anisotropy and the study by Wirjadi et al. [13]. The approach we present is closely related to many of the above referenced studies, and partly with the statistical approach based on mixtures of uniform and Gaussian models. Compared to previous work, this article contributes a physics-based definition of anisotropy of images and a set of anisotropy indices that are easy to compute, yet powerful enough and suited to the characterization of the textile materials. This article continues and details [14].

II. ANISOTROPY DEFINITION AND DETERMINATION

This Section presents a slightly different point of view of several issues presented in [14], with part of that study re-considered and recounted. All images processed and discussed in this article are from the personal database of the first author; the database was partly discussed in [14]. Also, the MATLAB program implementing the formula in this section is an improved version of the one discussed in [14].

There is no formal and unique definition of image anisotropy in the literature to our knowledge. Therefore, we feel compelled to state conditions that any definition of image anisotropy should satisfy. A set of intuitive conditions come to mind when defining anisotropy: (i) An image with spatially-uniformly distributed noise, $p(x,y) = ct.$, should have null anisotropy (or directivity factor equal to 1, anisotropy equal to directivity factor -1). (ii) A constant gray level image should have null anisotropy. (iii) An image of horizontal / vertical bars should have $\alpha \neq 0$. (iv) An image of horizontal / vertical asymmetric motives (tiles) should have $\alpha \neq 0$. (v) An image of horizontal / vertical symmetric motives should have $\alpha = 0$. (vi) The anisotropy measure should be invariant to the average brightness level of the image (a very difficult condition to satisfy). (vii) Spatially uniform additive noise should decrease the anisotropy value.

In [14], we argued that for determining anisotropy we need in the first place an adaptation of the concept in physics for images. A typical example in physics refers to the electrical properties of dielectrics, with the external electric field E resulting in an induced electric displacement $\vec{D} = \varepsilon_0 \vec{E} + \vec{P}$, $\vec{P} = [\chi]\vec{E}$, where $[\chi]$ is the electric susceptibility matrix, and ε_0 permittivity constant. The consequence of anisotropy is that the polarization and the external electric filed may not have the same direction. According to Encyclopædia Britannica [15], "*Anisotropy, in physics, the quality of exhibiting properties with different values when measured along axes in different directions.*" Merriam-Webster does not restrict the term for physics, "*exhibiting properties with different values when measured in different directions*" [16], yet the provided example refers to physics. In some previous studies, extensions of the anisotropy concept to images may be confusing by not making a distinction between anisotropy and asymmetry. In fact, one has to define what property of the image one measures, and how one measures it, for introducing anisotropy. There will be necessarily different values of anisotropy of an image, depending on the measured property. However, these definitions may be not similar in substance with the ones in physics, because there "measurement" should be interpreted as "relationship between action and effect" while for images apparently no action can be applied to them for studying the effect. Therefore, we revise the concept of image anisotropy, as stated in [14].

We differentiate between non-action (NA) anisotropy and action-related or effect anisotropy (E-anisotropy). The action may be a directional filtering, for example a differentiation (high pass filter), or an integration (low-pass filter), or combinations of them, along one axis. The measured effect may be the change in FFT spectrum, in wavelet spectra, in dispersion of the image projection functions (see below and [14]), or the changes in the spectra of the projection functions, or other derived measurements.

A concept of image anisotropy based on borrowing from physics the notion of different relations between action and effect on different directions, would be as follows [14]. Name ρ the "resistance"; when along the axis it will be denoted by $\rho_{||}$, along the orthogonal direction by $\rho_{\perp}$. In an image, the 'resistance" to an imaginary fluid flow is constituted by edges (fluid analogy). The larger is the length of an edge, the higher its flow resistance is. An image has anisotropy when $\rho_{||} \neq \rho_{\perp}$ (locally or globally). The anisotropy defined in [14] by $\alpha = \max proj_x(edges)/\max proj_y(edges)$, where $proj_x$ is the projection on Ox of the edges. The index α has several desirable properties: it is unitary for uniformly distributed noise, as well as for images of circles and for regular geometric figures with symmetry axes parallel to the coordinate ones [14].

Subsequently, we introduce several features of an image that may help defining anisotropy. The digital images used represent a color component of the original ones or the entire color image converted to gray-level and normalized to the interval [0, 255]. The resulted image is generically denoted by s_{ij}, where i,j are the pixel coordinate values. The image pre-processing includes contrast manipulations, filtering, segmentation, holes removal, and edge detection. The second section introduces the statistical tools used and their rationale. The statistical results on anisotropy and their sensitivity to the image processing methods are illustrated. The preprocessing first extracts the trend lines due to non-uniform illumination and smooth the lighting. This is possible for the images considered because they are supposed to represent a single material or a scene with a single type of object. Also, any portion of the image that is background is replaced with white. A median filter is applied to all original images and to the edge images.

Then, the projection functions on the two axes are computed for an image $s(i,j)$ (as in [14], slightly modified) as

$$h_x(i) = \frac{1}{N} \cdot \sum_{j=1}^{N} s(i,j); \quad h_y(j) = \frac{1}{N} \cdot \sum_{i=1}^{N} s(i,j), \quad (1)$$

where N is the dimension of the image, if it is square ($N \times N$), or $N = \min(N_x, N_y)$ if the image has dimension $N_x \times N_y$. In the last case, several such square $N \times N$ windows are computed. The projection functions $h_x(j), h_y(j)$ play a key role in this study. When it is needed to specify the image whose projections are computed, the notation h_x^s is used. The projection functions will be used for both the original image (after pre-processing) and the derived edge image, after the edges are extracted. Notice that the initial image is a matrix (when in gray level format), while the projections are vectors.

The following definitions and notations are used subsequently. The standard deviation of the vector $v(i)$ is denoted by σ_v or by $\sigma(v)$. The cross correlation between the vectors u and v, at shift k, is denoted by $C_{u,v}(k)$; we consider $k < N/2$. An edge image determined for an image $s(i,j)$ is denoted by $e^s(i,j)$. After edge detection, isolated bright pixels in 5×5 windows are removed with a simple filter according to the condition

$$if \sum_{h=-2}^{2} \sum_{k=-2}^{2} e_{i-h,j-k}^s < 300 \ then \ e_{ij}^s = 0. \quad (2)$$

Following [14], we use the indices of anisotropy:

$$\alpha_1^s = \frac{1}{255}\,\sigma(h_x^s)/\sigma(h_y^s), \quad \alpha_1^e = \sigma(h_x^e)/\sigma(h_y^e). \quad (3)$$

Notice that for non-isotropic images, $\alpha_1^e \approx 1$, according to the above definition of the anisotropy concept. The same anisotropy indices can be defined locally, on a square window of large enough dimension for the statistic is significant (preferably at least 7×7). In [14], we also proposed

$$\alpha = \sqrt{\sum_{i=1}^{N}\left(h_x(x_i) - h_y(y_i)\right)^2} \quad (4)$$

and several variations of it (including application to original and edge images). As well as an anisotropy factor determined by the spreading of the projection functions, according to

$$\alpha_x = \max_{\varphi}\left(\sigma\big(h_x(x)\big)\right), \quad \alpha_y = \sigma\big(h_y(x)\big) \quad (5)$$

where σ means standard deviation and the Ox axis is chosen in the direction that maximizes $\sigma\big(h_x(x)\big)$. Then one computes the ratio $\alpha = \alpha_x/\alpha_y$ as a measure of the anisotropy of the image.

Further, the anisotropy was computed based on the correlation of the projection functions, as

$$\alpha = \frac{1}{N} \cdot \frac{\max_m\left|Cor_{h_x,h_y}(m)\right| - \min_m\left|Cor_{h_x,h_y}(m)\right|}{\max h_x \cdot \max h_y} \quad (6)$$

where m is the shift in the correlation function. The value of α_4 when considering only the max of the correlation ranges between 0 and 1, with $\alpha = 1$ for $h_x = h_y$. This shows that the definition is not good for anisotropy, because a uniform picture has maximal anisotropy, while a pure noise has 0 anisotropy. Taking max-min, this issue is solved, because both uniform and uniform noise images have zero anisotropy. Notice that in the correlations one should consider 0-averaged h_x, h_y to obtain zero correlations for non-correlated functions. High values of the self-correlation of the projections at shifts different than zero point toward a periodicity in the respective direction. Except for the case of circular symmetry, periodicity means anisotropy. Finally, the value of the maximal correlation for various shifts of the two projections may indicate, for high values, a common periodicity on the two directions.

The edge images were obtained from the original using a parametric Sobel sedge extractor as described in [14], with various values of the parameter. The best values of the parameter were empirically found to be between 0.5 and 0.9. The anisotropy indices were computed for edge images obtained for k=0.5, k=0.7 and k = 0.9 and the average value of the indices so determined is considered.

III. RESULTS AND DISCUSSION

A MATLAB application was written [14] that performs sequentially the computation of the above defined indices for both the given images and their edge-determined counterparts. The edge detection is performed using the Sobel method available in MATLAB, combined with the method described in [17] for improving the edge detection (a few code

lines described in [17] were used). We used images from public databases of textile and texture pictures, but most of the tests were performed on our own database reported in [14].

We show two examples of results, one related to the application in textile charging, the other to the topic of the grant mentioned in the Acknowledgments. The original pictures are shown in Fig. 2; projections are in Fig. 1, for derived pictures in Fig. 3.
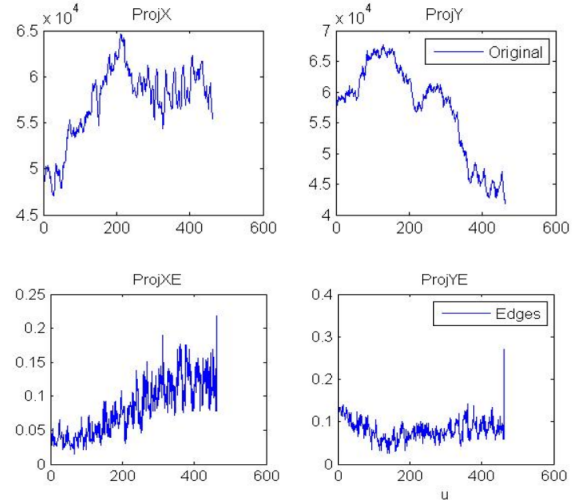

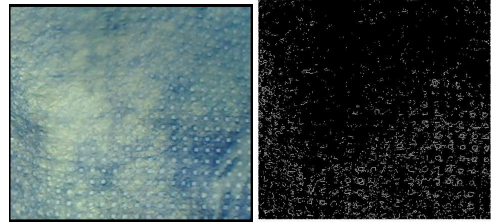Figure 1. Up: Projections original; Down: Projections Edges

Figure 2. Left: original picture; right: after edge extraction (k=0.9). Picture "PolyProp_Transparency_HNT_8"
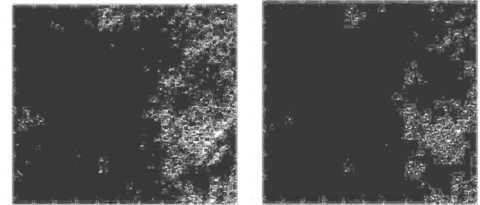

Figure 3. Original image; Right: same, filtered (median). Brightness and contrast modified for visibility

TABLE I. SUMMARY OF RESULTS FOR THE PICTURE "POLYPROP_TRANSPARENCY_HNT_8"

k	$\max(Cor_{h_x,h_y})/$ $max(h_x)max(h_y))$	$max(h_x)/$ $max(h_y)$	$std(h_x)/$ $std(h_y)$
Original	0.7477	0.9557	0.5304
0.1	0.4883	0.8069	1.1844
0.3	0.5289	0.8768	1.2269
0.5	0.3929	0.8119	1.4336
0.7	0.1144	0.808	1.5567
0.9	0.0628	0.8571	1.428

The next set of data is for a much degraded wall with several cracks ("Wall 1" picture in the database); see Figs. 4-6. A summary of results is shown in Table II.

IV. Conclusions and future work

The definition of the anisotropy introduced is concordant with the concept in physics and is intuitive. The related method for characterizing the anisotropy introduced in [14] and extended and perfected in this article is intuitive and simple to apply, with good statistical foundations; it is computationally intensive, but comparable to other methods in the literature.
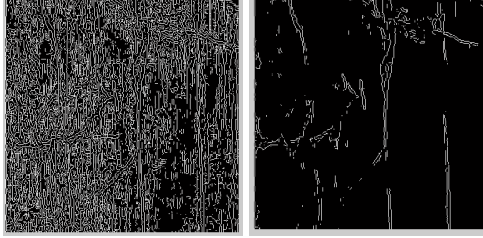

Figure 4.   Edge image with coefficient 0.1 (left) and 0.9 (right). Original image is a wall after bombardment (a small section from a picture on the Internet was processed)
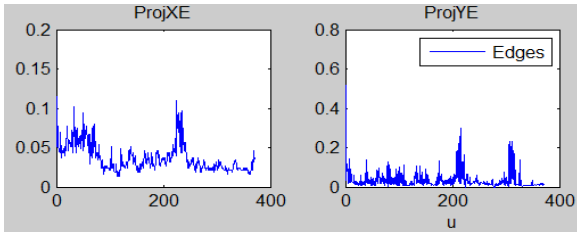

Figure 5.   Projections for edges obtained with k=0.9

TABLE II.   SUMMARY OF RESULTS FOR "WALL 1"

k	$\mathbf{max}(Cor_{h_x,h_y})/$ $max(h_x)max(h_y))$	$max(h_x)/$ $max(h_y)$	$\mathbf{std}(h_x)/$ $\mathbf{std}(h_y)$
0	0.8815	0.9422	0.4093
0	0.8815	0.9422	0.4093
0.1	0.2947	0.6146	0.3019
0.3	0.0989	0.4456	0.3245
0.5	0.0473	0.285	0.3523
0.7	0.0265	0.2228	0.3186
0.9	0.02	0.1606	0.2625

The results of the anisotropy assessment show consistency with the human's impression; moreover, the results are quite immune to the parameter of the edge extraction procedure and to small amounts of white noise. It is expected that the method can be used in a wide range of applications. In addition, the use of the Canny edge detector provides similar results.

In future work, the regression searched for, relating the electrostatic charging and the image of the material will have the form

$$q(i,j) = a\rho(i,j) + b\alpha(i,j) + c + \nu(i,j) \quad (7)$$

where a, b, c are constants, $q(i,j)$ is the charge density, $\rho(i,j)$ is the image density, α is anisotropy, and $\nu(i,j)$ is a noise accounting for random factors in the regression. The charge density is replaced by the electrical potential in the actual measurements. The constant b may include the effect of the angle between the vector of the main direction of anisotropy and the direction of the electrical charging of the material, as in the experiments reported in [1]. Results will be reported elsewhere.

References

[1]   H.-N. Teodorescu, L. Dascalescu, M. Hulea, M. C. Plopeanu, "Correlations between the electric charging properties and the optically determined structure of non-woven fabrics." Journal of Electrostatics, Vol. 71, Issue 4, Aug 2013, pp. 635–647.

[2]   M. Kass and A. Witkin, "Analyzing oriented patterns", Computer Vision, Graphics, and Image Processing, Vol. 37 Issue 3, Mar 1987, pp. 362 – 385.

[3]   B. Brunet-Imbault, G. Lemineur, C. Chappard, R. Harba and C.-L. Benhamou, "A new anisotropy index on trabecular bone radiographic images using the fast Fourier transform." BMC Medical Imaging 2005, 5:4 doi:10.1186/1471-2342-5-4

[4]   M.H. Keyhani, W.E. Hakimi, S. Wesarg, "Anisotropy correction of medical image data employing patch similarity." CBMS 2013, pp. 385-388.

[5]   T.S. Nguyen, S. Begot, F. Duculty, M. Avila. "Free-form anisotropy: A new method for crack detection on pavement surface images." 18th IEEE Int. Conf. Image Processing, Sep 2011, Bruxelles, Belgium.

[6]   H. Bierme and F. Richard, "Analysis of texture anisotropy based on some Gaussian fields with spectral density," Texture Analysis of Image Anisotropy, pp. 57-71.

[7]   F. Richard and H. Bierme. "A statistical methodology for testing the anisotropy of Brownian textures with an application to full-eld digital mammography." MAP5 2007-20. 2007.

[8]   H. Bierme, C.-L. Benhamou, and F. Richard, "Parametric estimation for Gaussian operator scaling random fields and anisotropy analysis of bone radiograph textures." In K. Pohl, (Ed.), Proc. Int. Conf. Med. Image Computing and Comp. Interv. (MICCAI'09), pp. 13–24, London, UK, Sep 2009.

[9]   S.G. Roux, M. Clausel, B. Vedel, S. Jaffard, P. Abry, "Self-similar anisotropic texture analysis: the hyperbolic wavelet transform contribution." IEEE Trans. on Image Processing, Vol. 22, no. 11, pp. 4353 – 4363, 2013.

[10]   S. Gabarda and G. Cristóbal, "Blind image quality assessment through anisotropy." JOSA J. Opt. Soc. Am. A, Vol. 24, Issue 12, pp. B42-B51 (2007) doi: 10.1364/JOSAA.24.000B42

[11]   R. Lehoucq, J. Weiss, B. Dubrulle, A. Amon, A. Le Bouil, J. Crassous, D. Amitrano and F. Graner, "Analysis of image vs. position, scale and direction reveals pattern texture anisotropy", Frontiers in Physics, Jan 2015, Vol. 2, Article 84.

[12]   L.J. van Vliet and P.W. Verbeek, "Estimators for orientation and anisotropy in digitized images." ASCI'95, Proc. 1st Conf. Advanced School Computing and Imaging, Heijen, The Netherlands, May 16-18, 1995, pp. 442-450.

[13]   O. Wirjadi, K. Schladitz, A. Rack, T. Breuel, "Applications of anisotropic image filters for computing 2d and 3d-fiber orientations. Stereology and image analysis." ECS10 – Proc. 10th Eur. Congress ISS, (V. Capasso et al. Eds.), MIRIAM Project Series, ESCULAPIO Pub. Co., Bologna, Italy, 2009.

[14]   H.-N. Teodorescu, "Defining Indices of Image Anisotropy and an Image Data-Base for Testing the Anisotropy Detection." Submitted.

[15]   anisotropy. (2016). In *Encyclopædia Britannica*. Retrieved from http://www.britannica.com/science/anisotropy

[16]   Definition of anisotropic. http://www.merriam-webster.com/dictionary/anisotropic

[17]   "Detecting a cell using image segmentation" ttp://www.mathworks.com/help/images/examples/detecting-a-cell-using-image-segmentation.html.